Journal of Alloys and Compounds 745 (2018) 532–537

Contents lists available at ScienceDirect

Journal of Alloys and Compounds

journal homepage: http://www.elsevier.com/locate/jalcom

Crack initiation mechanism in lanthanum-doped titanium-zirconium-molybdenum alloy during sintering and rolling

Ping Hu [a, b, *], Yu-hang Zhou [a, b], Jie Deng [a, b], Shi-lei Li [a, b], Wen-jing Chen [a, b], Tian Chang [a, b], Bo-liang Hu [a, b], Kuai-she Wang [a, b], Peng-fa Feng [c], Alex A. Volinsky [d]

[a] School of Metallurgy Engineering, Xi'an University of Architecture and Technology, Xi'an 710055, China
[b] National and Local Joint Engineering Research Center for Functional Materials Processing, Xi'an University of Architecture and Technology, Xi'an 710055, China
[c] Jinduicheng Molybdenum Co., Ltd., Xi'an 710077, China
[d] Department of Mechanical Engineering, University of South Florida, Tampa FL 33620, USA

ARTICLE INFO

Article history:
Received 20 September 2017
Received in revised form
13 February 2018
Accepted 14 February 2018
Available online 16 February 2018

Keywords:
Lanthanum-doped titanium-zirconium-molybdenum alloy
Crack mechanism
Secondary phase particles
Microstructure
Fracture

ABSTRACT

Lanthanum-doped titanium-zirconium-molybdenum (La-TZM) alloy was prepared by powder metallurgy and rolling process. The processing crack and crack initiation mechanisms of La-TZM alloy after sintering, hot rolling and cold rolling were studied by scanning and transmission electron microscopy. The results show that the doped $La(NO_3)_3$, TiH_2 and ZrH_2 have finer secondary phase in the La-TZM alloy plate. The fracture mode of sintering billet is inter-granular, but the fracture surface of hot rolling exhibited transgranular cleavage. However, the cold rolling is quasi-cleavage fracture. The secondary phase particles tend to hinder the movement of dislocations causing dislocations pile-up. The resulting tensile stress can accelerate cracks nucleation and growth, and the crack propagation will be deflected by the secondary phase particles. The crack initiation can be avoided by reducing local stress concentration caused by dislocations.

1. Introduction

Molybdenum is a refractory rare metal with a melting point of 2620 °C. Molybdenum alloy is widely used in missiles, high temperature heating elements, turbines and fusion reactor components, as well as electrical and electronic manufacturing equipment, aerospace, metal processing, extrusion and forging molds due to its the high strength, creep resistance, thermal conductivity and other properties [1,2]. However, molybdenum has a body-centered cubic crystal structure with less independent slip systems and higher ductile-to-brittle transition temperature, which limit further processing [3–5]. Alloying is an effective way to improve mechanical properties of pure molybdenum and alloys, including TZM and rare earth doped molybdenum alloys. Lanthanum-doped titanium-zirconium-molybdenum (La-TZM) alloy (0.5% Ti, 1% La, 0.06–0.12% Zr and 0.01–0.04% C) has good mechanical properties. Compared with pure molybdenum, La-TZM alloy has high recrystallization temperature, low ductile-to-brittle transition temperature, excellent high temperature strength, low temperature ductility and good welding properties [6–13].

Mechanical properties, high temperature oxidation resistance, corrosion resistance and fracture mechanisms of molybdenum and its alloy have been discussed previously [6–15]. The ultimate strength of the La-TZM alloy is 1405 MPa at room temperature [11]. For the same processing conditions, lanthanum doping has significantly improved tensile strength and elongation, which increased by 28.2% and 32.8%, respectively, and the ductile-to-brittle transition temperature of the La-TZM alloy was decreased to −120 °C, which is 40 °C lower than for the TZM alloy [12]. The recrystallization starting temperature of the La-TZM alloy is 1500 °C, which is 300 °C higher than for the TZM alloy [15]. Only a few research reports focus on the crack initiation in La-TZM alloys during deformation processing. This research group has successfully prepared high-performance La-doped molybdenum by powder metallurgy methods under high temperature and pressure, however, cracks occurred during sintering and rolling. In this paper, the crack initiation mechanism in the La-TZM alloy during sintering and

* Corresponding author. School of Metallurgy Engineering, Xi'an University of Architecture and Technology, Xi'an 710055, China.
E-mail address: huping1985@126.com (P. Hu).

https://doi.org/10.1016/j.jallcom.2018.02.191
0925-8388/

Table 1
Chemical element composition of pure molybdenum powder (μg/g).

O	N	C	Pb	Bi	Sn	Sb	Cd	Fe	Al	Si	Mg	Ni	Cu	Ca	P	Mo
150	15	5	0.5	0.5	0.5	1	1	5	1.5	2	2	3	1	1.5	1	bal.

Table 2
Sintering procedure of the La-TZM alloy.

Temperature, °C	Heating time, h	Holding time, h
30–400	2	2
400–900	3.5	2
900-1250	2	1
1250–1600	1.5	2
1600–1950	2	3.5
furnace cooling		

rolling was studied by observing microstructure evolution. The purpose of this study is to improve the La-TZM alloy quality during the sintering and rolling process, and to increase production volume.

2. Experimental procedure

The La-TZM alloy plate was prepared by mixing, pressure sintering and rolling. La-TZM powders include pure molybdenum powder with chemical composition listed in Table 1, titanium hydride powder (0.5%), zirconium hydride powder (0.08%), lanthanum trioxide (1%) powder and organic carbon source (fructose). The alloy was doped with Ti and Zr elements using the solid-solid method, and La with C were doped into the Mo-Ti-Zr alloy powder by the solid-liquid method. Then the mixed powders were milled in the planetary ball mill at 40 rpm for 2 h, and the ball-to-powder weight ratio was 2:1, while the diameter of molybdenum balls was 10 mm. Powder was filled into the die mold using the YT79-500 hydraulic press by compression molding with 180 MPa pressure for 20 min. Sintering was performed in the HM3002 intermediate frequency induction furnace in 99.99% hydrogen environment. The temperature of sintering was 1950 °C for 3.5 h. The sintering process had 5 temperature plateaus, and lasted for about 10.5 h. The sintering procedure is shown in Table 2.

The thickness of sintering billet was 12 mm, and the rolling process included hot and cold rolling, and the finished plate thickness was 0.5 mm after cold rolling. The cracks were analyzed in the sintered billet and rolled plate. Several cracked samples of the sintered billet, hot and cold rolled plate after polishing and corrosion testing were observed by scanning electron microscopy (SEM, JSM-6390), and the surrounding components of the crack were obtained from the energy dispersive spectrometry (EDS) data. Microstructure observations of the cold rolled plate were carried out by transmission electron microscopy (TEM, JEM-200CX).

3. Results and discussion

3.1. Cracks microstructure characteristics of the sintered billet

The sintered billet of the La-TZM alloy cracked during the powder metallurgy process. Fig. 1 shows SEM images of the microstructure and the fracture surface of the sintered La-TZM alloy. It shows the whole crack with the source of the crack found in Fig. 1a. Fig. 1b shows that the fracture mode is intergranular

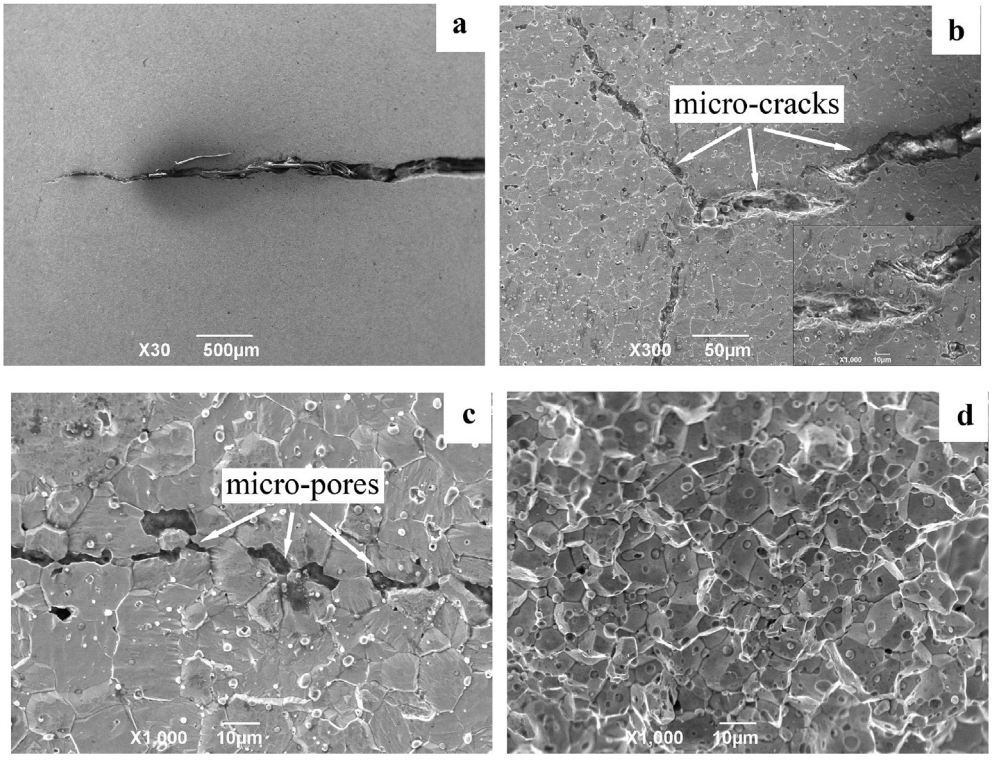

Fig. 1. SEM images of sintering La-TZM alloy crack: (a) macro-crack; (b) micro-crack; (c) micro-pores; (d) fracture surface.

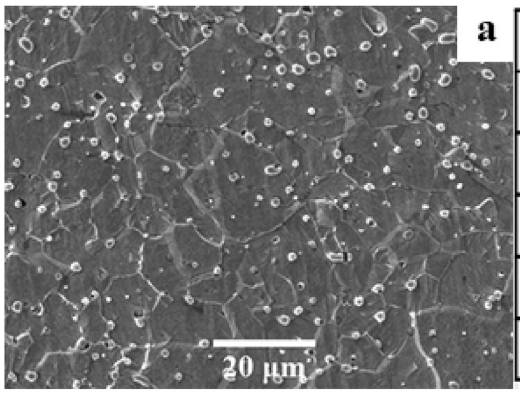

element	W%	X%
O	6.76	30.15
Ti	1.51	2.25
Zr	1.22	0.95
Mo	87.50	65.10
La	3.01	1.55

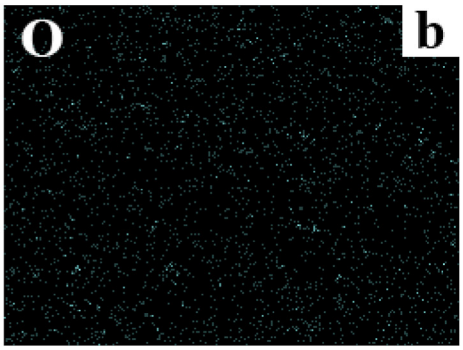

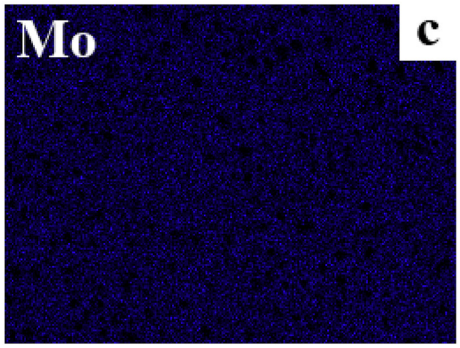

Fig. 2. SEM image and EDS analysis of sintering La-TZM alloy.

fracture. Fig. 1b and c show that the secondary phase particles are uniformly distributed in the grains and along the grain boundaries. The sintered billet surface has some pores, and residual pores are created at grain boundaries during the sintering neck formation. The micro-crack is not continuous, but the crack propagation path does not change. Fracture surface is smooth with no plastic deformation in Fig. 1d. The as-sintered alloy exhibits typical intergranular fracture. From the experimental results, it is concluded that many pores at grain boundaries are aggregated to form cracks. Decreased grain boundary bonding force is caused by segregation of solute atoms at grain boundaries, causing grain boundary cracks [16]. In addition, oxygen is distributed throughout the sintered billet with an atomic content of 30.15%. Grain boundaries and secondary phase particles show higher oxygen content by scanning electron microscopy in Fig. 2. Thus, these alloys showed intergranular fracture due to oxygen segregation at grain boundaries [17].

3.2. Cracks and microstructure of hot and cold rolled plate

Fig. 3 shows SEM image and EDS data of precipitated phases in the La-TZM alloy after hot and cold rolling. The thickness was 3 mm and 0.6 mm by hot rolling and cold rolling, respectively. In Fig. 3a and b the crack propagation path is deflected when it encountered the secondary phase particles with 3–5 μm size. The reason is that the crack tips and the micropores around the micron-size secondary phase particles rapidly shear crack along the slip lines, and the two will connect together finally. Fig. 3b and c shows that the micro-pores are formed around the secondary phase particles (1 μm small size and 3–5 μm large size), and then create conditions for crack nucleation. Fig. 3a–c shows inclusions in the area near the crack of the hot rolled plate, and the secondary phase particles are distributed around the crack, based on the energy dispersive spectrometry analysis results. In addition, highly active Ti and Zr atoms originating from dehydrogenation of TiH_2 and ZrH_2 at 500 °C react with oxygen to form TiO_2, Ti_2O_3, ZrO_2 and $Mo_xTi_yO_z$. Meanwhile, lanthanum is present in the form of La_2O_3 in the secondary phase particles [5,18], which corresponds to the EDS analysis in Fig. 3. Fig. 4 shows the secondary phase particles located inside the grains and at grain boundaries. Similarly, Fig. 3d and e shows that the secondary phase particles about 1 μm in size are distributed near the crack in the cold-rolled La-TZM alloy. This is due to the fact that the micro-pores are first formed at the secondary phase particles or the interface of the secondary phase particles with the substrate when the material is loaded to a certain extent, and then the secondary phase particles tend to hinder the movement of dislocations and cause dislocations pileup, and the resulting tensile stress will accelerate the nucleation and propagation of cracks [19].

In Fig. 5a, there are striped dislocations around the secondary phase particles in the cold rolled plate observed by transmission electron microscopy. A large number of dislocation pile-up groups have a large stress concentration, so the cracks are most susceptible to nucleation around defects (micro-pores, secondary phase particles, etc.). Fig. 5b shows that the dislocations are hindered when they pass through the secondary phase particles. The secondary phase particles are wrapped around a large number of dislocations.

As shown in Fig. 6b, when the applied external stress is large enough, the dislocation pileup at the secondary phase particles is resumed, meanwhile, dislocations at the grain boundaries are hindered from movement to form dislocation pile-ups. Fig. 6c shows that dislocations move towards the secondary phase particles, and the micro-voids are formed when the accumulated elastic strain is sufficient to overcome the interface bond strength between the secondary phase particles and the matrix material to produce a new surface; the phenomenon of local stress concentration produced at the grain boundaries. In Fig. 6d, cleavage cracks are initiating at the grain boundaries and the micro-voids are growing to reduce the high stress concentration when the stress

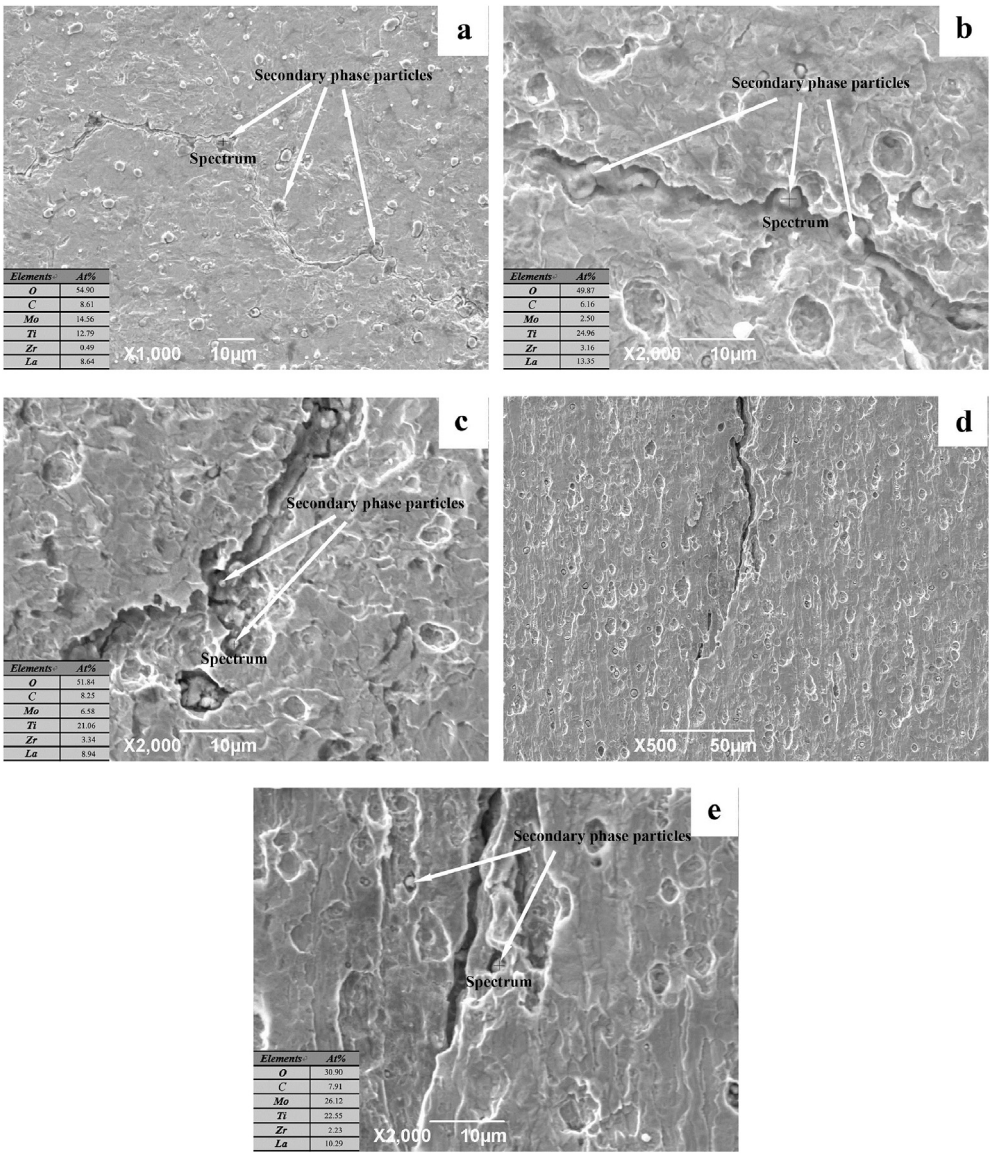

Fig. 3. SEM image and EDS analysis of the precipitated phases of the as-rolled La-TZM alloy (a), (b), (c): hot rolling; (d) and (e): cold rolling.

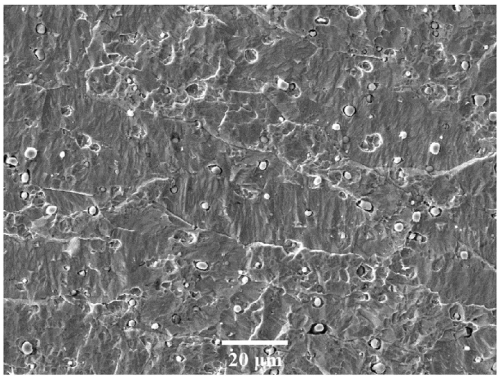

Fig. 4. SEM image of the hot rolled La-TZM plate.

reaches its critical value at dislocation pile-ups. Fig. 4e shows cleavage cracks at grain boundaries joining together with the micro-voids to form cracks. Gurland and Plateau shows that the interface will crack by releasing the strain energy to produce a new surface when the elastic strain energy of the particles at the time of loading can reach the surface forming energy [20]. The corresponding energy criterion can be expressed as:

$$\eta\sigma = (E\gamma/d)^{1/2} \quad (1)$$

where σ is the applied stress, η is stress concentration factor, γ is interfacial fracture energy, E is modulus of elasticity and d is particle diameter. From Equation (1), it can be concluded that the larger the secondary particle size, the easier the nucleation of the crack.

3.3. Fractography analysis

Fig. 7 shows the fracture morphology of hot and cold rolled plates of the La-TZM alloy observed by SEM. After rolling, the grains elongate, transform and brake along the rolling direction. There was a different height of cleavage surface of hot rolled plate fracture morphology, which exhibited brittle fracture by transgranular cleavage in Fig. 7a. As seen in the fracture morphology of the cold

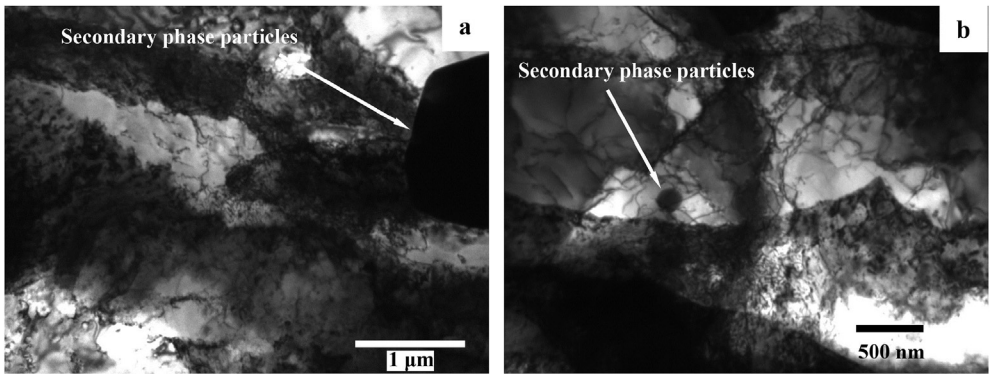

Fig. 5. TEM images of the La-TZM alloy secondary phase particles after cold rolling: (a) micron-sized; (b) nano-sized.

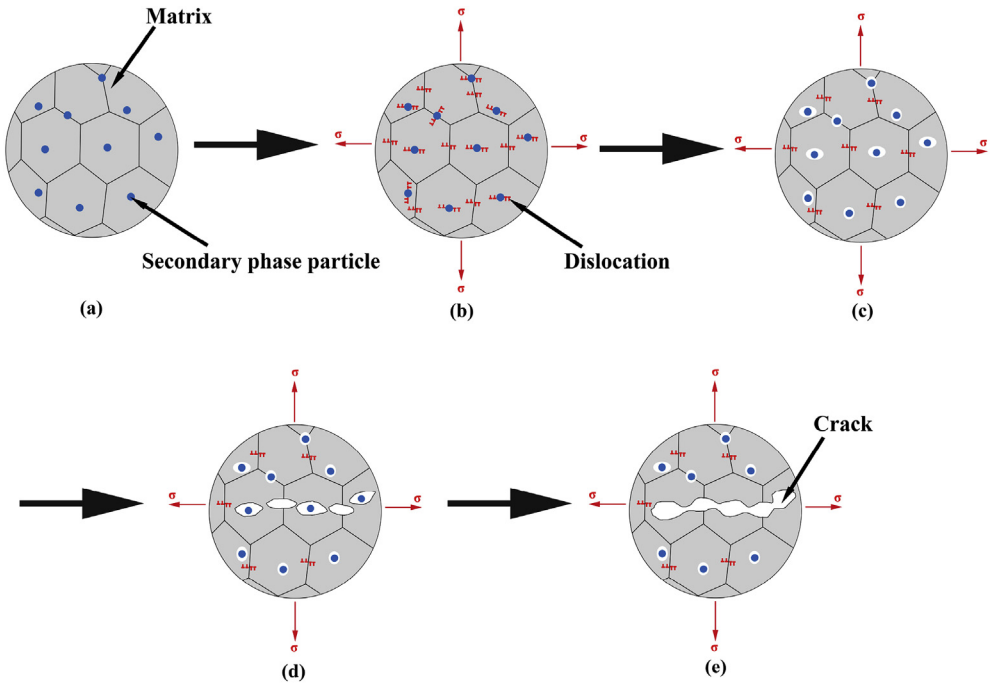

Fig. 6. Schematic diagram of crack formation mechanism in the La-TZM alloy.

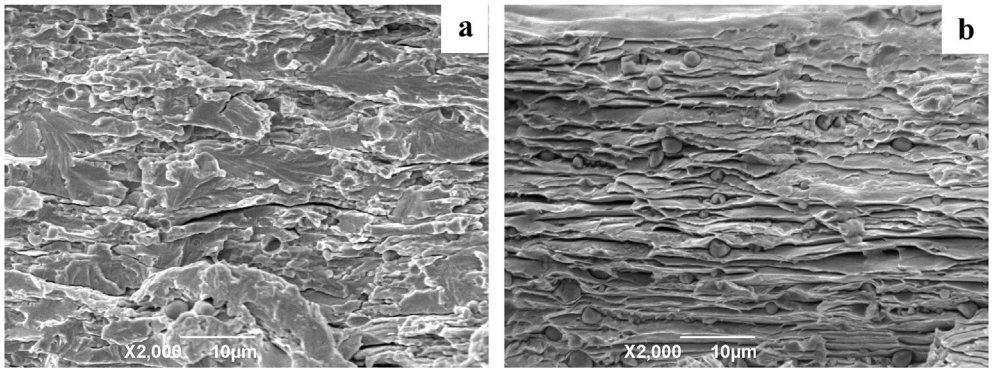

Fig. 7. SEM images of fracture morphology of the La-TZM alloy: (a) hot-rolled plate; (b) cold-rolled plate.

rolled plate in Fig. 7b, there are characteristics of cleavage surface and toughness tear, which is a mixture of cleavage and quasi-cleavage fracture. There is a large amount of secondary phase particles in the lamellar fibrous structure, and the secondary phase particles absorb energy to form cracks when the stress is concentrated.

Crack initiation and propagation are usually associated with the secondary phase particles or inclusions in material, and several major stages of crack behavior are: a) The interface between the secondary phase particles or the particles themselves are cracked to produce microvoids in the high strain area; b) The micro-pores grow around the particles under plastic strain and hydrostatic pressure; c) Micro-porous aggregation is due to the interaction between microvoids or between micro-pores and cracks to produce necking [19]. Therefore, though stress analysis, choosing reasonable rolling reduction and annealing process can effectively reduce local stress concentration caused by dislocations and avoid cracks.

4. Conclusions

(1) The as-sintered La-TZM alloy exhibited typical intergranular fracture with the aggregated micro-pores at grain boundaries forming cracks.
(2) Secondary phase particles and grain boundaries are distributed near the crack in the La-TZM alloy plate, and tend to hinder the movement of dislocations, and cause dislocation pileup, thus resulting in tensile stress causing nucleation and propagation of cracks.
(3) Cracks are most susceptible to nucleation at defects (micro-pores, secondary phase particles, etc.).
(4) Hot rolled plate fracture morphology exhibited brittle fracture by transgranular cleavage. Cold rolled plate fracture morphology is quasi-cleavage fracture.

Acknowledgements

This work was supported by the National Key Research and Development Program of China (2017YFB0305600, 2017YFB0306000), China Postdoctoral Science Foundation (2016M600770), the Science and Technology Coordinating Innovative Engineering Project of the Shaanxi province (2015KTZDGY09-04) and the Service Local Special Program of Education Department of the Shaanxi Province, China (16JF016).

References

[1] S.P. Chakraborty, S. Banerjee, K. Singh, I.G. Sharma, A.K. Grover, A.K. Suri, Studies on the development of protective coating on TZM alloy and its subsequent characterization, Mater. Proc. 207 (2008) 240–247.
[2] E. Ahmadi, M. Malekzadeh, S.K. Sadrnezhaad, Preparation of nanostructured high temperature TZM alloy by mechanical alloying and sintering, Int. J. Refract. Met. H 29 (2011) 141–145.
[3] S.P. Chakraborty, S. Banerjee, I.G. Sharma, A.K. Suri, Development of silicide coating over molybdenum based refractory alloy and its characterization, Nucl. Mater. 403 (2010) 152–159.
[4] G. Filacchioni, E. Casagrande, U.D. Angelis, G.D. Santis, D. Ferrara, Effects of strain rate on tensile properties of TZM and Mo–5%Re, Nucl. Mater. 307–311 (2002) 705–709.
[5] G. Liu, G.J. Zhang, F. Jiang, X.D. Ding, Y.J. Sun, J. Sun, E. Ma, Nanostructured high-strength molybdenum alloys with unprecedented tensile ductility, Nat. Mater. 3544 (2013) 344–350.
[6] F. Yang, K.S. Wang, P. Hu, H.C. He, X.Q. Kang, H. Wang, R.Z. Liu, A.A. Volinsky, La doping effect on TZM alloy oxidation behavior, J. Alloys Compd. 593 (2014) 196–201.
[7] X.Q. Kang, K.S. Wang, Z. Zhang, P. Hu, H.C. He, R.Z. Liu, P.Z. Wang, Effect of lanthanum doping method on properties of La-TZM alloy, Rare Metal Mater. Eng. 5 (2015) 1254–1258.
[8] P. Hu, K.S. Wang, F. Yang, H.C. He, X.Q. Kang, H. Wang, Z.T. Yu, J.F. Tan, Preparation and oxidation behavior of La-TZM alloy plates, Rare Mater. Eng. 7 (2014) 1722–1726.
[9] H.C. He, K.S. Wang, P. Hu, X.Q. Kang, P.Z. Wang, R.Z. Liu, Effects of rare earth La element doping on recrystallization behavior of TZM alloy sheet, Rare Mater. Eng. 5 (2015) 1297–1300.
[10] P. Hu, K.S. Wang, F. Yang, H.C. He, X.Q. Kang, H. Wang, Z.T. Yu, J.F. Tan, Preparation and properties of La-TZM alloy by substitution of organic carbon for graphite, Rare Mater. Eng. 6 (2014) 1502–1506.
[11] P. Hu, F. Yang, J. Deng, T. Chang, B.L. Hu, J.F. Tan, K.S. Wang, W.C. Cao, P.F. Feng, H.L. Yu, High temperature mechanical properties of TZM alloys under different lanthanum doping treatments, J. Alloys Compd. 711 (2017) 64–70.
[12] P. Hu, F. Yang, K.S. Wang, Z.T. Yu, J.F. Tan, R. Song, B.L. Hu, H. W, H.C. He, A.A. Volinsky, Preparation and ductile-to-brittle transition temperature of the La-TZM alloy plates, Int. J. Refract. Met. Hard Mater. 52 (2015) 131–136.
[13] H.C. He, K.S. Wang, P. Hu, X.Q. Kang, P.Z. Wang, R.Z. Liu, Fracture and microstructure of La doped TZM plate, Rare Mater. Eng. 4 (2014) 964–967.
[14] B.V. Cockeram, The role of stress state on the fracture toughness and toughening mechanisms of wrought molybdenum and molybdenum alloys, Mater. Sci. Eng. A 528 (2010) 288–308.
[15] K.S. Wang, J.F. Tan, P. Hu, Z.T. Yu, F. Yang, B.L. Hu, R. Song, H.C. He, A.A. Volinsky, La_2O_3 effects on TZM alloy recovery, recrystallization and mechanical properties, Mater. Sci. Eng. A 636 (2015) 415–420.
[16] H. Tawancy, A.U. Hamid, N. Abbas, Practical Engineering Failure Analysis, CRC Press, Florida, 2004.
[17] K. Babinsky, J. Weidow, W. Knabl, A. Lorich, H. Leitner, S. Primig, Atom probe study of grain boundary segregation in technically pure molybdenum, ScienceDirect 87 (2014) 95–103.
[18] J.L. Fan, M.Y. Lu, H.C. Cheng, J.M. Tian, B.Y. Huang, Effect of alloying elements Ti, Zr on the property and microstructure of molybdenum, Int. J. Refract. Met. Hard Mater. 27 (2009) 78–82.
[19] T. Anderson, Fracture Mechanics: Fundamentals and Applications, CRC press, Florida, 2005.
[20] J. Gurland, J. Plateau, The mechanism of ductile rupture of metals containing inclusions, Trans. ASM 56 (1963) 442–454.